BNL-67573

Predicting Particle Critical Supersaturation from Hygroscopic Growth Measurements in the Humidified TDMA. Part II: Laboratory and Ambient Studies

FRED J. BRECHTEL* AND SONIA M. KREIDENWEIS

Department of Atmospheric Science, Colorado State University, Fort Collins, Colorado

(Manuscript received 21 October 1998, in final form 22 July 1999)

ABSTRACT

Laboratory studies are used to test the method proposed in Part I for estimating the critical supersaturation of quasi-monodisperse, dry particles from measurements of hygroscopic growth at relative humidities below 100%. An advantage of the proposed technique is that it directly links dry particle size to cloud condensation nuclei (CCN) activity and simultaneously provides some information on particle chemical composition. Studies have been conducted on particles composed of NaCl, $(NH_4)_2SO_4$, NH_4HSO_4, internally and externally mixed NaCl–$(NH_4)_2SO_4$, and on ambient particles of unknown chemical composition. A modified form of the Köhler equation is fit to measurements from a humidified tandem differential mobility analyzer to derive two chemical composition–dependent parameters and the critical supersaturation for a given dry particle size. A cloud condensation nucleus counter is used to simultaneously observe the critical supersaturation of the same dry particles.

Results show that for particles composed of single salts and for diameters between 32 and 57 nm, the average agreement between critical supersaturations derived from measurements of hygroscopic growth and theoretical values of S_{crit} is -13% ($1\ \sigma = 8.5\%$, $n = 9$). This agreement is similar to experimental uncertainties in critical supersaturations determined from laboratory studies on particles of known chemical composition. The agreement between values of S_{crit} predicted by the fit technique and CCN study-derived values is poorer (-6% to -65%) for ambient particles. This is likely due to both changes in ambient particle characteristics during the study and limitations in the modified Köhler model derived in this work.

1. Introduction

The cloud nucleating ability of an aerosol particle is frequently expressed in terms of S_{crit}, its critical supersaturation (Hudson et al. 1998; Pruppacher and Klett 1997). At relative humidities above S_{crit} the droplet can spontaneously grow by addition of water. In general, S_{crit} depends on both particle size and composition, and some studies have directly linked aerosol size to S_{crit} (Covert et al. 1998; Fitzgerald et al. 1982; Hudson 1982). Many studies relating chemical composition to cloud nucleating ability have relied on bulk chemical samples and assumptions about particle homogeneity (e.g., Svenningsson et al. 1994; Covert et al. 1998).

This paper outlines the experimental methods and results of laboratory studies where values of S_{crit} are derived for known-size, monodisperse particles composed of NaCl, $(NH_4)_2SO_4$, NH_4HSO_4, internally and externally mixed NaCl–$(NH_4)_2SO_4$, and ambient particles of known size and unknown chemical composition. For particles of known composition, S_{crit} is determined three ways: by theoretical calculation, from measurements using a thermal gradient diffusion cloud chamber cloud condensation nucleus (CCN) counter, and by fitting the modified Köhler model derived in Part I of this work to hygroscopic growth observations from a humidified tandem differential mobility analyzer (HTDMA; Rader and McMurry 1986). The results from quality control experiments to verify proper equipment operation are presented. Observed hygroscopic growth is compared to published results and theoretical calculations in order to validate HTDMA operation. Values of S_{crit} derived from HTDMA results are compared to theoretical values and to values derived from CCN counter measurements to test the proposed technique for deriving S_{crit} from observed hygroscopic growth.

The eventual goal of this work is to develop the capability to link particle size and S_{crit} for ambient aerosol size distributions of unknown composition. To this end, a version of a general and thermodynamically consistent model of the osmotic coefficient has been incorporated into the modified Köhler equation derived in Brechtel and Kreidenweis (2000, hereafter Part I). In principle, if sufficiently many monodisperse particle populations

* Current affiliation: Environment Chemistry Division, Brookhaven National Laboratory, Upton, New York.

Corresponding author address: Sonia Kreidenweis, Dept. of Atmospheric Science, Colorado State University, Fort Collins, CO 80523.
E-mail: soniak@aerosol.atmos.colostate.edu

© 2000 American Meteorological Society

of different sizes were sampled, representative of the total size distribution, the values of S_{crit} for each population could be determined and the concentration of particles that are CCN at each S_{crit} (the CCN spectrum) could be derived. In practice, CCN spectra were not derived in this work, primarily due to the long sampling times the CCN counter required to measure the value of S_{crit} against which the HTDMA-derived value could be compared.

A few studies of ambient particles of unknown composition are performed as a ''first test'' of the proposed technique on more complex particles. However, the potential effects of soluble gases and slightly soluble compounds within the ambient particles, as pointed out by Schulmann et al. (1996) and Laaksonen et al. (1998), are not explicitly accounted for in the current version of the modified Köhler model. The primary purpose of the current study is to examine the ability of the proposed technique to derive S_{crit}, and to compare the errors for known particle composition with those for unknown composition.

2. Experimental approach

In Part I of this work, a modified form of the Köhler equation for a droplet containing a single solute that completely dissociates in solution was derived under three fundamental assumptions: 1) the partial molar volume of water could be replaced by the molar volume of pure water in the Kelvin term, 2) the surface tension of the droplet solution could be replaced by the surface tension of pure water in the Kelvin term, and 3) the osmotic coefficient could be replaced by a less complex parameterization that depended on only two unknown parameters and still exhibited the correct thermodynamic limiting behavior for dilute solutions. The form of the derived Köhler equation is [Eq. (33) from Part I of this work]

$$\mathrm{RH} = 100\ \exp\left[\frac{4\sigma_w M_w}{\rho_w R T D_{\mathrm{drop}}}\right] \times \exp\left[\frac{-M_w c}{1000}\left(Y_f - \frac{A_\phi c^{1/2} Y_f^{3/2}}{\sqrt{2} + b_{\mathrm{pit}} c^{1/2} Y_f^{1/2}} + 2c\beta_{0,f} Y_f^2\right)\right]. \tag{1}$$

In the above equation, M_w is the molecular weight of water, R is the universal gas constant, and b_{pit} is a fit parameter from Pitzer's model of the osmotic coefficient Φ. These parameters are constants. The droplet size is D_{drop}, RH is the relative humidity, and T is the temperature. These parameters are measured during HTDMA studies. The surface tension of pure water is σ_w, ρ_w is the density of pure water, and A_ϕ is the Debye–Hückel parameter for Φ. Note that σ_w, ρ_w, and A_ϕ are a function of T only. The term c is defined as

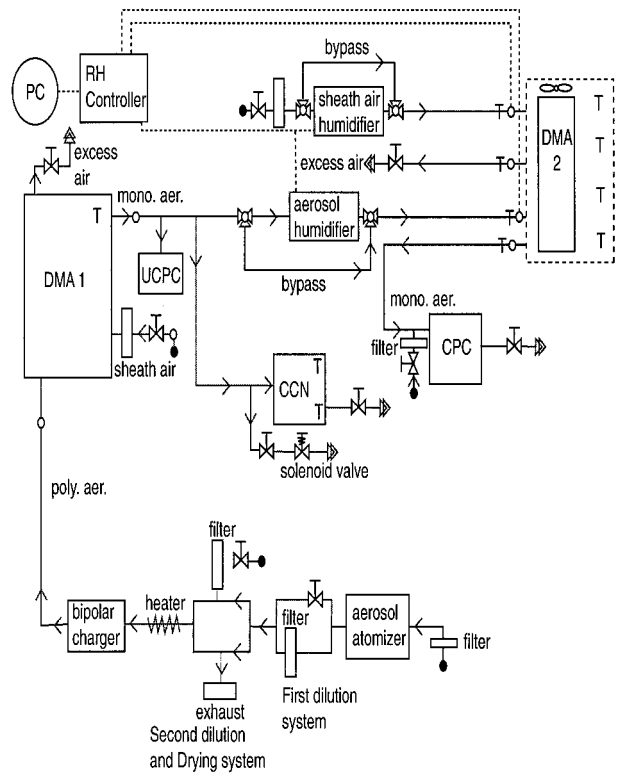

FIG. 1. Schematic diagram of HTDMA system. Solid lines with arrows designate air sample flow pathways. Solid dot designates particle-free compressed air source. Double triangle designates vacuum source. Open dot designates RH sensor. ''T'' designates location of thermistor temperature measurement.

$$c = \frac{1000 D_{p,\mathrm{sol}}^3}{\rho_w (D_{\mathrm{drop}}^3 - D_{p,\mathrm{sol}}^3)}, \tag{2}$$

where $D_{p,\mathrm{sol}}$ is the dry particle size and is measured during HTDMA studies. This leaves Y_f and $\beta_{0,f}$ as the two, chemical composition–dependent unknowns that remain to be determined. By fitting Eq. (1) to measured (D_{drop}, RH) data pairs from HTDMA studies, the two unknowns can be determined and Eq. (1) used to calculate the maximum equilibrium RH, which is defined as S_{crit}.

a. HTDMA measurement system

The hygroscopicity of submicrometer particles can be investigated as a function of size using the humidified tandem differential mobility analyzer technique (Rader and McMurry 1986). A schematic diagram of the HTDMA system is shown in Fig. 1. The polydisperse aerosol is first exposed to ions in a radioactive charge neutralizer so that the charge distribution on the sampled aerosol is known as a function of size (Wiedensohler 1988). In the HTDMA, dry (RH $<$ 10%), quasi-monodisperse particles are selected from the polydisperse, input size distribution using a differential mobility an-

alyzer (DMA). The DMA selects particles based upon their electrical mobility. The relationship between electrical mobility and particle size is given by

$$Z_p = \frac{neC_c}{3\chi\pi\nu_{\text{air}}D_p}, \tag{3}$$

where Z_p is the electrical mobility, n is the number of charges carried by the particle, e is the elementary electric charge, C_c is the Cunningham correction factor, χ is a shape factor that accounts for nonspherical particles (Hinds 1982), and ν_{air} is the dynamic viscosity of air (Kinney et al. 1991). The electric field voltage in the first DMA is kept constant in order to select a constant, dry, monodisperse particle size. Each DMA was operated with the aerosol sample inlet flow equal to the aerosol sample outlet flow. Sheath flow rates between 6.9 and 10 times the aerosol flow rate were used in the first DMA and the sheath airflow rate was five times the aerosol flow rate in the second. Therefore, the width of the sampled mobility window was between ±10% and ±14.4% of the centroid mobility for DMA1 and ±20% for the second DMA.

The concentration of particles exiting the first DMA was measured with an ultrafine condensation particle counter (UCPC; model 3025, TSI Incorporated, St. Paul, Minnesota). Particles exiting the first DMA were exposed to controlled RHs between 80% and 92% before entering the second DMA. The sheath airflow RH of the second DMA was controlled to agree with the aerosol inlet flow RH of the second DMA within 1%. Relative humidity sensors (Humitter 40, Vaisala Inc., Woburn, Massachusetts) were calibrated over saturated salt solutions before and after HTDMA studies using the results of Greenspan (1977). Results from the RH calibrations indicated that RH measurements for all HTDMA studies exhibited an accuracy between ±0.8% and ±1% RH and a precision of ±0.85%. The second DMA was housed in a Plexiglass enclosure to maintain constant temperature and RH conditions. The maximum temperature gradient in DMA2 measured using precision thermistors (model 44030, YSI Inc., Yellow Springs, Ohio) was 0.1°C, corresponding to a maximum 0.6% change in RH at the standard operating temperature of 29.5°C. If the particles take up water, they will grow in size and exhibit a lower electrical mobility in the second DMA. A condensation particle counter (CPC; model 3010, TSI Incorporated) is used to count the particles exiting the second DMA as the voltage in that DMA is scanned. By observing the electrical mobility where the CPC measures the maximum number of particles, the size of the wetted particles can be determined, and the water content derived from the difference between the wet and dry sizes. By controlling the conditioner and second DMA humidities at several different values, the growth as a function of relative humidity may be determined for each input, dry monodisperse particle population. Between 6 and 15 size bins were used to resolve the grown droplet size distribution.

A TSI model 3760 Constant Output Atomizer (TSI Incorporated) was used to generate particles of known chemical composition for all studies except those on ambient particles. Salt solutions were made by combining a known volume of nanopure water with a known mass of salt. A compressed air source was used to generate the atomizer flow, dilution system flow, and both sheath airflows in the DMAs used in the HTDMA system. All airflows generated from the compressed air source were passed through HEPA filters and a coalescing filter with a carbon membrane to remove oil droplets and organic vapors. The atomizer and dilution system airflows were dried to RHs between 2% and 10% using in-line Drierite columns (W. C. Hammond Incorporated, Xenia, Ohio). The atomizer produces on the order of 10^8 particles cm^{-3}; therefore, it was necessary to dilute the output flow with dry, particle-free air with a dilution ratio of 10:1.

b. Cloud condensation nucleus counter

The CCN counter is used to measure the number concentration of dry particles activated to cloud droplets at a given supersaturation. The model M1 Cloud Condensation Nucleus Counter (DH Associates, Tucson, Arizona) used in this study was the same unit used by Cruz and Pandis (1997) in their studies of the CCN activity of organic compounds. The unit consists of a thermal gradient diffusion chamber, a laser used to illuminate the droplets formed inside the chamber, a video camera to image the illuminated droplets, and electronics to digitize and count the droplets in the captured images. The top and bottom surfaces of the diffusion chamber are kept saturated with liquid water and are separated by a glass cylinder so the laser may be used to illuminate droplets formed between the two plates. A thermoelectric cooler is used to cool the bottom plate, while the top plate temperature is allowed to equilibrate with the room temperature. When the bottom plate is cooled, a linear temperature gradient is created between the two plates. Both surfaces are kept at 100% RH, and since the saturation vapor pressure of water depends exponentially on temperature, the linear temperature gradient produces a quasi-parabolic water vapor supersaturation profile between the two plates. Although the maximum supersaturation between the plates cannot be measured directly, it can be calculated from the measured top and bottom plate temperatures using Eq. (4):

$$S_{\max} = 100\frac{\rho_s(T_t) + \rho_s(T_b) - 2\rho_s\left[\dfrac{T_t + T_b}{2}\right]}{2\rho_s\left[\dfrac{T_t + T_b}{2}\right]}, \tag{4}$$

where T_t and T_b are the top and bottom plate temperatures, respectively, and ρ_s is the water vapor density at saturation for the indicated temperature. The laser

passes through the glass ring and is directed through the chamber so that its position coincides with the location of maximum supersaturation in the chamber. Particles are introduced into the chamber by a pump that draws 1.5 L min^{-1} for 5 s through the chamber from the same monodisperse outlet flow of DMA1 sampled by DMA2 of the HTDMA system. The sample flow is drawn through the chamber so that the particles enter through the top plate and later exit through a hole in the bottom plate. The 5-s pumping time is sufficient to draw 125 cm^3 of air through the chamber. The chamber volume is 100 cm^3. After the 5-s pumping time, an additional 5 s are allowed for the supersaturation profile to be reestablished. The remaining 20 s of the 30-s sampling period are used to obtain video images of droplets within the laser beam in the chamber. The sensing volume is determined by the diameter of the laser and by the length along the laser viewed by the video camera. The volume and data processing algorithm are set by the manufacturer and cannot be changed. The sensing volume is 0.006 cm^3, and one sample takes 0.5 min; therefore, to sample a full cubic centimeter of air, 83.3 min are required. The extremely small sample volume has important ramifications with respect to counting statistic uncertainties. The images are digitized and processed to remove spurious counts by the software within the instrument. Once processed, the number of droplets counted in the beam, the current accumulated 0.1 cm^3 counts, and the current accumulated 1 cm^3 counts of droplets are read and stored by a data acquistion system.

At droplet concentrations around 1000 cm^{-3}, the video imaging system cannot resolve all of the individual droplets in the laser beam and the droplet number actually counted is reduced due to the coincidence of droplets in the sensing volume. Tabulated corrections for this effect have been provided by the manufacturer and were applied during data processing. The correction amounts to $\approx$10% for droplet concentrations near 1000 cm^{-3}. Particle losses in the CCN counter were also quantified and are described below.

3. Results

a. Validation of HTDMA operation

In order to validate proper HTDMA sizing and operation, three types of experiments were performed. The first type of experiment quantified potential particle contamination. To examine the potential contamination due to leaks, the system was operated with no solution in the atomizer and filtered air as the sample flow. Observed artifact particle number concentrations were two and five orders of magnitude smaller than those observed during experiments where ambient and laboratory particles were sampled, respectively. The observed artifact particles were also found to have diameters smaller than 30 nm, smaller than the sizes selected during HTDMA studies. Therefore, contamination due to leaks was found to be insignificant. To examine possible contamination from impurities in the nanopure water used to mix the salt solutions, nanopure water with no added solute was atomized and the size distribution measured using DMA1 and the UCPC. Artifact particles were observed from the atomized nanopure water solution. The observed size distribution was found to exhibit a mode size near 30 nm, a geometric standard deviation of 1.6, and a number concentration (before DMA1) of 7000 cm^{-3}. The measurement was repeated with similar results. The concentrations of artifact particles in the 40–60-nm size range, representative of particles sampled in HTDMA studies on known composition particles, was between 180 and 450 cm^{-3}. For comparison, the range of concentrations of 40–60-nm salt particles sampled during HTDMA studies was two orders of magnitude higher than the observed concentration of artifact particles. Therefore, some fraction of the total number concentration of atomized salt particles may have contained impurities from the nanopure water. Based on the low relative monodisperse number concentrations of the particles resulting from impurities in the nanopure water, the assumption is made that they did not significantly influence the results of HTDMA growth or CCN activity studies conducted for this work.

The second type of experiment was intended to quantify the systematic oversizing of the TDMA system, as found by previous investigators (Rader and McMurry 1986). The humidity system was bypassed and dry particle size distributions were measured. These studies were performed on particles in the 40–100-nm size range composed of ammonium sulfate and sodium chloride. For 25 size distribution scans performed on 40-nm NaCl particles, the average mode diameter determined by fitting a lognormal curve to the number concentration data from DMA2 was 40.9 nm. The standard deviation of the average mode diameter was 0.13 nm, resulting in a coefficient of variation in the mean size of 0.33%. The ratio of the average mode size from DMA2 to the mean diameter selected by DMA1 was 1.02, or a systematic oversizing of 2% was found in the TDMA for 40-nm particles. This is consistent with previous results from Rader and McMurry (1986). Similar results were obtained with ammonium sulfate particles. Studies performed on 50-nm $(NH_4)_2SO_4$ particles indicated that the oversizing decreased to around 1%. At 60 nm, the systematic oversizing again decreased to 0.7%. At 100 nm, no systematic oversizing was observed. Given that the systematic oversizing in the TDMA amounts to a very small correction for droplet sizes between 60 and 200 nm measured by DMA2, HTDMA data were not corrected for this effect. HTDMA studies on dry 40-nm particles demonstrated that the sizing precision of the system was $\pm$0.33%.

The third type of experiment involved controlled, elevated RH droplet growth studies on NaCl and $(NH_4)_2SO_4$ particles with diameters between 25 and 60 nm. The goal was to compare experimentally deter-

TABLE 1. Summary of all HTDMA and CCN studies conducted for this work. Study numbers designate day of year of study and are used in text to designate particular studies.

Chemical compostion	D_p range (nm)	HTDMA study numbers	Number of RH scans	CCN study numbers
		Single solutes		
Ammonium sulfate	25–102	161, 162 169, 176	85	74*, 75*, 147, 148, 162, 169, 176
Sodium chloride	37–96	146, 163 164	49	76, 77, 152, 163, 164
Ammonium bisulfate	40	172, 178	43	172, 178
		Mixed solutes		
Internally mixed NaCl–$(NH_4)_2SO_4$	32	173	16	173
Externally mixed NaCl–$(NH_4)_2SO_4$	37–40	177, 181	47	177, 181
		Ambient samples		
Unknown	65–120	174, 175 182	42	174, 175, 182
Total studies		15	282	22

* Two CCN studies conducted on this day.

mined droplet growth with theoretical predictions from the reference Köhler model and with results of electrobalance measurements of droplet growth by Tang and Munkelwitz (1994). A summary of all HTDMA and CCN studies conducted for this work is given in Table 1. Study numbers in the table designate the day of year (DOY) of the study. The results from all studies on NaCl and $(NH_4)_2SO_4$ particles are shown in Fig. 2. In Fig. 2, the solid line designates theoretical growth curves calculated using the reference Köhler model described in

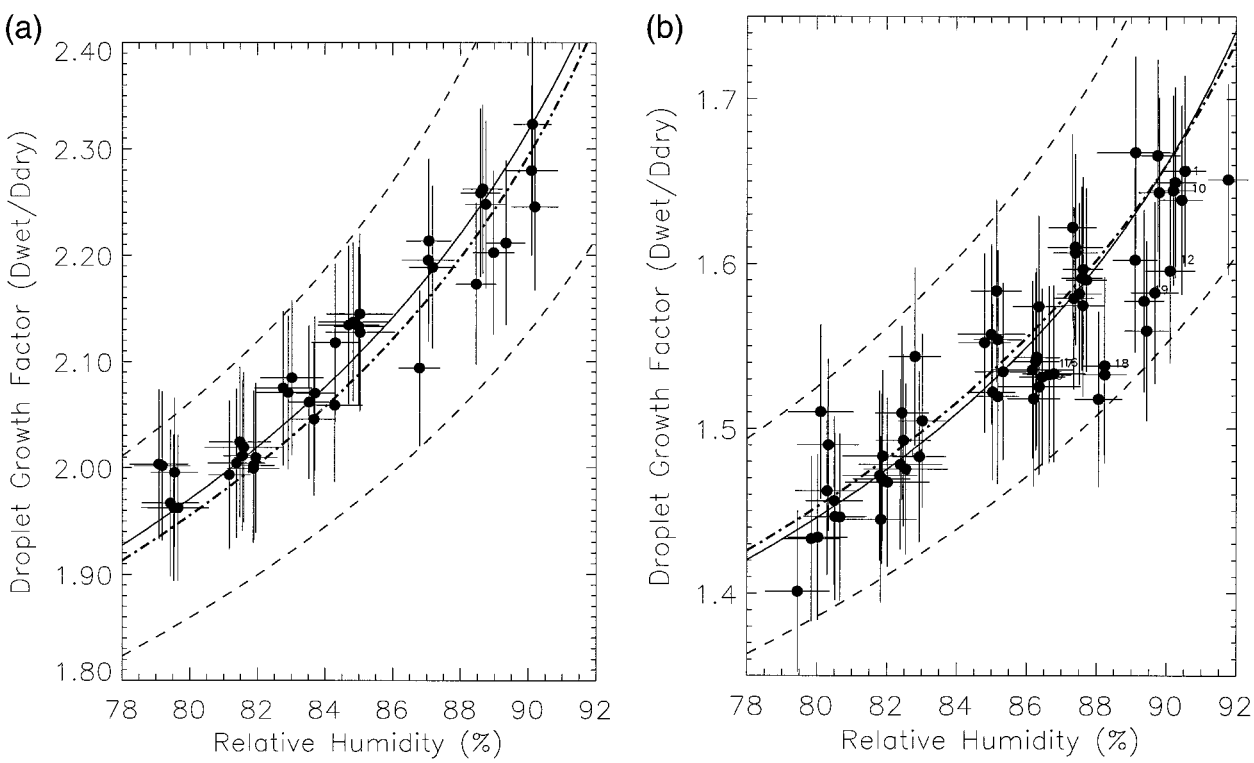

FIG. 2. (a) Hygroscopic growth study results from all HTDMA experiments conducted on NaCl particles. Solid line designates RH calculated using the reference Köhler model. Thick dashed–dot line represents results from Tang and Munkelwitz (1994) for NaCl particles. Dashed lines represent two times the standard deviation in the average error between observed and theoretical growth factors added and subtracted from the dashed–dot line. Experimental data are designated by solid dots. Vertical uncertainty bars represent a ±3.5% uncertainty in the observed growth factor. Horizontal uncertainty bars are calculated using the observed standard deviations in the sheath, monodisperse inlet, and monodisperse outlet RHs, and the 0.5% RH uncertainty attributable to the RH sensor calibration procedure. (b) As in (a) except for $(NH_4)_2SO_4$ particles.

Part I, which uses the Pitzer and Mayorga (1973) model for the osmotic coefficient. The thick dashed–dot line is the theoretical growth curve using a_w computed from polynomials from Tang and Munkelwitz (1994). The measured average HTDMA study temperature was used in the theoretical RH calculations. Experimental points are shown as solid dots; the vertical and horizontal bars designate calculated uncertainties in the measurement RH and particle and droplet sizes. The RH measurement uncertainties were determined by calculating the root mean square sum of the standard deviations of the sheath, monodisperse inlet, and monodisperse outlet flow RHs in the second DMA, as well as the $\pm 0.5\%$ RH uncertainty attributable to the RH sensor calibration procedure. A $\pm 2\%$ uncertainty was assumed as a conservative estimate for droplet and dry particle size uncertainties, producing a $\pm 3.5\%$ overall uncertainty in the droplet growth factor. Due to the cubic shape of NaCl particles, a shape factor (χ) of 1.08 was used to convert the dry particle electrical mobility diameter to the Stokes diameter, as suggested by Kelly and McMurry (1992). No shape factor was applied to the diameter of $(NH_4)_2SO_4$ dry particles. The dashed lines represent the 2 σ value in the percent agreement between observed and theoretical growth ratios ($\pm 3.5\%$). The 2 σ value has been added to and subtracted from the droplet growth curve from the results of Tang and Munkelwitz (1994). In processing the results from these studies it was found that the RH of the monodisperse inlet flow to DMA2 had to be controlled within 2% of the sheath flow RH and that the standard deviations of both RHs had to be less than 1% in order for accurate growth measurements to be made. HTDMA results not satisfying the above RH control criteria were deemed unacceptable. Applying these criteria resulted in the rejection of 17% of HTDMA study results.

Results in Fig. 2a for NaCl show excellent agreement with both theoretical growth curves. An uncertainty of $\pm 5\%$ was reported by Rader and McMurry (1986) in their growth ratio measurements on NaCl particles using the HTDMA technique. Berg et al. (1998) report a $\pm 3\%$ error in HTDMA-derived growth factors, attributable to counting statistics and RH fluctuations inside the DMAs. For HTDMA studies on NaCl particles, the average percent agreement between observed and theoretical growth factors is 0.6% ($1\ \sigma = 1\%$, $n = 40$). The average percent agreement between observed and theoretical RH and D_{drop} values are -1.2% [($1\ \sigma = 1.4\%$, $n = 40$)] and 0.5% [($1\ \sigma = 1.8\%$, $n = 40$)], respectively.

Results in Fig. 2b for $(NH_4)_2SO_4$ also show very good agreement with theory; however, there is a slight trend to underestimate growth at RHs above 88%. For HTDMA studies on $(NH_4)_2SO_4$ particles, the average percent agreement between observed and theoretical growth factors is -0.3% ($1\ \sigma = 1.1\%$, $n = 63$). The average percent agreement between observed and theoretical RH and D_{drop} values are 0.2% [($1\ \sigma = 1.6\%$, $n = 63$)] and -0.8% [($1\ \sigma = 1.8\%$, $n = 63$)], respectively. A likely explanation for the lower observed growth of $(NH_4)_2SO_4$ particles at higher RHs is the smaller relative DMA1 dry size selected during some of the elevated RH $(NH_4)_2SO_4$ runs compared to other studies. Studies with dry particle sizes smaller than 35 nm are labeled in Fig. 2b with the study number. The smaller DMA1 dry size may have resulted in an increased penetration of relatively smaller particles through Brownian diffusion, contributing to the underestimated droplet growth factor. Nevertheless, the droplet growth factors observed in this study are within experimental agreement with the theoretical values and serve to validate the capability of the HTDMA system to accurately measure particle hygroscopic growth for RHs between 80% and 92%.

b. Validation of CCN counter operation

Preliminary studies with the CCN counter showed that the number concentrations of activated droplets were no more than 80% of the input particle number concentrations for dry particle sizes and compositions where all of the particles should have acted as CCN. Therefore, the total particle losses in the CCN counter sample line, solenoid valve, and top plate inlet were determined experimentally for particle sizes between 15 and 250 nm by measuring the monodisperse particle concentration in the diffusion chamber with a CPC, while the first DMA monodisperse outlet flow concentration was simultaneously measured with the UCPC. The CPC sampled from the CCN diffusion chamber through a modified ring assembly. Results from the particle loss study are shown in Fig. 3. For particle diameters between 15 and 250 nm, between 26% and 76% of the particles counted by the UCPC entered the CCN chamber. Over 90% of the observed particle loss is due to losses inside the CCN counter, with the remainder due to diffusional losses in sample tubing. A polynomial fit for the particle penetration as a function of diameter is shown in Fig. 3. The size-dependent losses were accounted for in determining the correct value of the input dry particle concentration (N_{ucpc}) to use in calculating the ratio of the droplet concentration measured by the CCN counter (N_{ccn}) to N_{ucpc}.

To validate proper operation of the CCN counter, the activation supersaturations of $(NH_4)_2SO_4$, NH_4HSO_4, and NaCl particles were investigated for chamber supersaturations between 0.2% and 1.0%. The purpose of these studies was to evaluate the experimental uncertainties in the techniques for deriving experimental values of S_{crit} and also to verify the repeatability of the method. A total of 16 runs were performed using two different experimental techniques. The first technique involved sampling progressively smaller, monodisperse particles with the CCN counter set for a constant chamber supersaturation. The diameter where 50% of the input particles were activated to droplets ($D_{act,50}$) could be determined by fitting a sigmoidal function to the ratio of N_{ccn} to N_{ucpc} versus particle diameter. Using the ex-

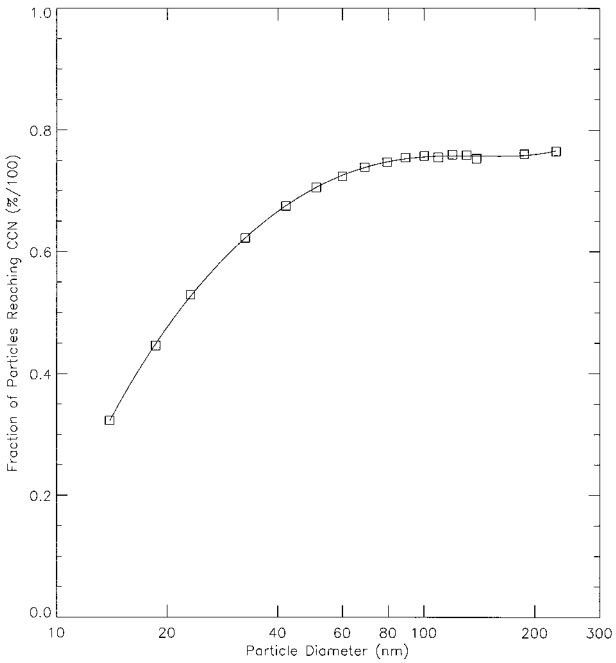

FIG. 3. Fraction of particles reaching CCN chamber due to diffusional losses and losses in solenoid valve and top plate inlet in CCN counter as a function of particle size.

perimentally determined value of $D_{act,50}$ and the known chemical composition, the theoretical value of S_{crit} could be calculated and compared to the average chamber maximum supersaturation for the experiment calculated from Eq. (4). A total of 10 studies of this type were performed. UCPC data were corrected for sample line losses and for losses inside the CCN counter. CCN data were corrected for coincidence errors and the 0.1 cm^3 data were averaged to determine the droplet number concentration for either a full cubic centimeter of air sampled by the CCN counter, or after 400 droplets had been counted, whichever came first.

The second method for deriving S_{crit} from CCN measurements involved maintaining a constant input, monodisperse particle size, and varying the chamber supersaturation so that values of the ratio of N_{ccn} to N_{ucpc} between 0.2 and 0.9 could be observed. The supersaturation where the ratio of N_{ccn} to N_{ucpc} was equal to 0.5 was then defined as the experimental estimate of S_{crit}. Although both methods for deriving S_{crit} are equally valid for evaluating experimental uncertainties in derived S_{crit} values for particles of known composition, the second method was employed for all simultaneous HTDMA–CCN studies after and including DOY 163. This choice was based on the fact that for ambient particles of unknown chemical composition, only the second method will allow valid experimental estimates of S_{crit} to be made.

Figure 4a shows results from a CCN study conducted on DOY 152 using the first method and NaCl particles. The chamber was set for a supersaturation of 0.255% and the chamber supersaturation exhibited a standard deviation of $\pm 0.018\%$ over the course of the measurement. Experimental data are shown as squares in the figure. The particle size corresponding to the point where 50% of the input dry particles were activated to droplets and counted as CCN was determined by fitting a sigmoidal function to the ratio of N_{ccn} to N_{ucpc}. From the fit results, the observed value of $D_{act,50}$ was 59 nm. The theoretical value of S_{crit} for a 59-nm NaCl particle at the average chamber temperature is 0.263%. For this run, the experimental estimate of S_{crit} is 3% lower than the theoretical value.

Results from a CCN study conducted on DOY 169 using the second method where the chamber supersaturation was varied are shown in Fig. 4b. Experimental data are shown as asterisks and the solid line represents the best-fit line to the data. The sigmoidal function was not used because of the sparsity of data points; the approximately linear portion of the function has been fit instead. Between 1 and 2 h were required for the chamber supersaturation to stabilize after being reset. The same amount of time was required to measure a significant number of droplets at a given supersaturation. Therefore, the 2–4-h period required for each chamber supersaturation limited the number of points that could be obtained. For the study shown in Fig. 4b, the input monodisperse size to the CCN chamber was kept constant at 57.2 nm, and the particles were composed of $(NH_4)_2SO_4$. The theoretical value of S_{crit} for this size and composition particle is 0.41%, and is shown in Fig. 4b as the small solid dot. The experimentally determined value of S_{crit} shown in Fig. 4b by the intersection between the dotted line and the x axis, was 0.42%. The agreement between theoretical and experimental values of S_{crit} is 3%. For chamber supersaturations between 0.3% and 0.54% for this study, the standard deviation in chamber supersaturation was less than 0.005% for each of the four different chamber supersaturations examined. The other symbols in Fig. 4b are described below.

The best estimate of the accuracy of derived S_{crit} values is determined by averaging the percent differences between theoretical and experimental values of S_{crit} for all CCN studies on known composition particles, shown in Fig. 5. The theoretical value of S_{crit} shown in Fig. 5 for the externally mixed results is the average of the theoretical S_{crit} values for the sampled NaCl and $(NH_4)_2SO_4$ particles. For all CCN studies conducted on known composition particles at supersaturations below 0.8%, the agreement between theory and experiment is very good. The calculated average percent agreement is -0.6%, with a standard deviation of 11% ($n = 16$). The vertical error bars represent the $\pm 22\%$ confidence interval value in S_{crit}. The precision in cloud condensation nucleus counter (CCNC)-derived values of S_{crit} was determined by pooling results from three sets of two replicate measurements of S_{crit} conducted on $(NH_4)_2SO_4$, NH_4HSO_4, and externally mixed NaCl–$(NH_4)_2SO_4$ par-

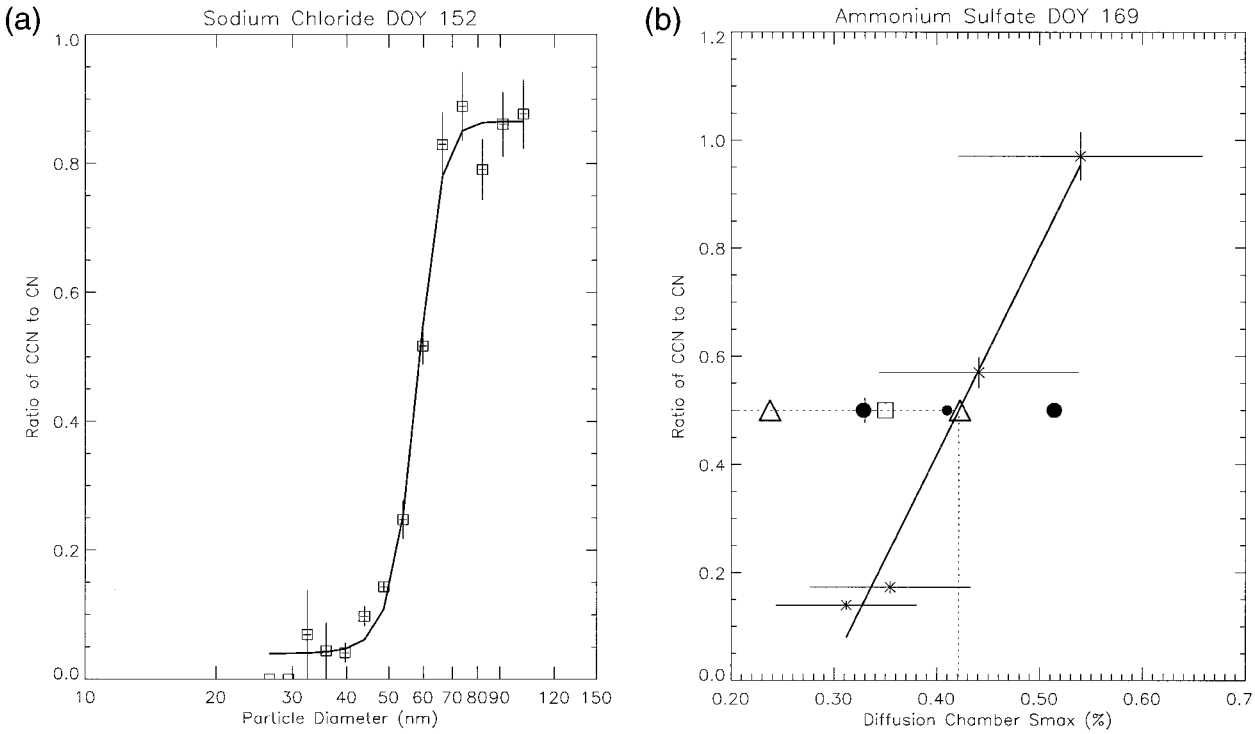

FIG. 4. (a) CCN validation study results for NaCl particles on DOY 152. Solid line designates fit of sigmoidal function to experimental data designated by squares. Vertical uncertainty bars represent Poisson counting error in CCN droplet concentration. The nominal CCN chamber supersaturation was 0.26%. The confidence interval for CCNC-derived values of S_{crit} is ±22%. (b) CCN validation study results for 57.2-nm $(NH_4)_2SO_4$ particles on DOY 169. Solid line designates best-fit line to experimental data designated by asterisks. Vertical uncertainty bars represent Poisson counting error in CCN droplet concentration. Horizontal uncertainty bars represent the ±22% confidence interval in S_{crit}. Triangles designate the ±28% confidence interval in S_{crit} values predicted by fit routine from HTDMA growth results. Square represents value of S_{crit} from the fit with all data pairs and no applied error, while the plus symbol represents the value from the fit with applied error. Dotted lines designate experimentally observed values of S_{crit}. The small solid dot represents the theoretical value of S_{crit} for a 57.2-nm-diameter $(NH_4)_2SO_4$ particle. Larger solid dots represent the ±22% confidence interval in CCNC-derived values of S_{crit}.

ticles with the same diameter (Skoog et al. 1992). The confidence interval, expressed as the ratio (multiplied by 100) of the pooled standard deviation in S_{crit} divided by the smallest average value of S_{crit} from the pooled datasets, is ±22% at the 95% confidence level.

c. *Comparison of measured, HTDMA-derived, and theoretical values of S_{crit} for particles composed of single solutes*

Having validated the operation of the HTDMA system and the CCN counter, we now examine the values of S_{crit} derived from HTDMA studies and compare them to those from simultaneous CCN studies and to theoretical values.

Hygroscopic growth results for NaCl and $(NH_4)_2SO_4$ were shown in Fig. 2. The (D_{drop}, RH) data pairs were input to the fit routine with the modified Köhler model, Eq. (1), to derive S_{crit}. The fit routine was run on all available data pairs, with and without applied random errors to the input data. The results from the fit routine for studies on NaCl, $(NH_4)_2SO_4$, and NH_4HSO_4 are shown in Table 2. In Table 2, the dry particle size and derived values of Y_f, $\beta_{0,f}$, S_{crit}, and D_{crit} are listed. Also shown are the errors in S_{crit} and D_{crit} derived from the fit routine relative to theoretical values calculated using the reference Köhler model described in Part I of this work. The χ^2 convergence value of the fit is shown in Table 2 in units of percent RH. For each HTDMA study and chemical composition there are two rows in Table 2. The first row represents results where no errors were applied to the input data pairs. The second row for each composition in Table 2 shows the average results of 20 runs of the fit routine where random errors were applied to the input data. The purpose of the fitting runs with applied errors was to test the sensitivity of derived values of S_{crit} to variations in the data input to the fit routine. The applied random errors were between ±2% for $D_{p,sol}$ and D_{drop}. The random errors for the input RH values were calculated for each HTDMA RH as the root-mean-square sum of the experimental uncertainty in the RH measurement and the standard deviations in the DMA2 RHs during the HTDMA scan due to fluctuations in RH control. The maximum applied RH errors were between ±1%.

From Table 2, the agreement between theoretical and HTDMA-derived values of S_{crit} is between 6% and −24%. The greater disagreement for the first NaCl study

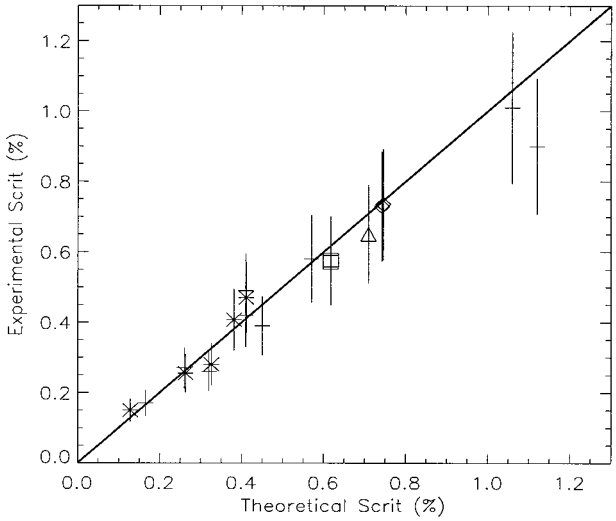

FIG. 5. Comparison of values of S_{crit} determined from all CCN studies in this work and theoretical values of S_{crit} calculated using the reference Köhler model for the temperature conditions of each CCN study. Solid line is 1:1 line and designates perfect agreement between theory and experiment. Symbols represent the following: plus for $(NH_4)_2SO_4$, asterisk for NaCl, diamond for NH_4HSO_4, triangle for internally mixed NaCl–$(NH_4)_2SO_4$, and squares for externally mixed NaCl–$(NH_4)_2SO_4$. The confidence interval for CCNC-derived values of S_{crit} is $\pm 22\%$.

shown in Table 2 is most likely due to the fact that this was one of the earliest HTDMA studies and the RH control was not as good as during later studies. The error analyses summarized in Table 2 are shown for one run in Fig. 4b. The square in the figure represents the value of S_{crit} from the fit routine using all data pairs as input and no applied error, while the plus symbol (behind leftmost solid dot) represents the value with applied error. The large solid dots represent the $\pm 22\%$ confidence interval in CCNC-derived values of S_{crit} about the experimentally determined value of S_{crit}. For all of the studies shown in Table 2, the average agreement between HTDMA-derived and theoretical values of S_{crit} is -13% with a standard deviation of 8.5% ($n = 10$). Using the techniques outlined in Skoog et al. (1992), the confidence interval for a 95% confidence level can be calculated for the HTDMA-derived values of S_{crit}. The confidence interval expressed as a percent error in S_{crit} was found to be $\pm 28\%$, similar to the value of $\pm 22\%$ found for CCNC-derived values of S_{crit}. The $\pm 28\%$ confidence interval in HTDMA-derived S_{crit} values is shown in Fig. 4b as the large triangles. The HTDMA-derived values of S_{crit} and D_{crit} demonstrate reasonable agreement with theory. It is evident from both the figure and tabulated results that the fit routine tends to underpredict the value of S_{crit}. This underprediction of S_{crit} is due primarily to the overestimate of values of the osmotic coefficient by the parameterization of Φ used in the modified Köhler model. Larger disagreement between theoretical and HTDMA-derived values of S_{crit} is found for NH_4HSO_4. The disagreement is similar to that found in numerical studies on particles composed of NH_4HSO_4 and is due to the fact that the proposed parameterization for Φ is less accurate for this compound than is the full Pitzer model itself (Kim et al. 1993).

It is of interest to compare the derived values of Y_f with the theoretically perfect values listed in Table 4 of Part I of this work. Numerical studies indicate that the sensitivity of the fit routine results to the value of $\beta_{0,f}$ is much less than that to the value of Y_f; therefore, we only compare values of Y_f. We note that, although the values of Y_f are similar for $(NH_4)_2SO_4$ and NH_4HSO_4, the value for NaCl is between 1.4 and 3 times greater than those for $(NH_4)_2SO_4$ and NH_4HSO_4. Values of Y_f for NaCl, $(NH_4)_2SO_4$, and NH_4HSO_4 derived from the fit routine agree with theoretically perfect values within -17%, -15%, and 7%, respectively, suggesting that useful information concerning the chemical composition of the sampled particles may be derived from the fit routine parameters.

Finally, we examined how the choice of different subsets of the total set of (D_{drop}, RH) data pairs influences the agreement between theoretical and HTDMA-derived values of S_{crit}. Values of S_{crit} as much as 45% lower than

TABLE 2. Summary of theoretical S_{crit} values, Y_f and $\beta_{0,f}$ fit parameters, and D_{crit} values determined HTDMA study results on particles composed of single solutes. The confidence interval of HTDMA-derived values of S_{crit} is $\pm 28\%$. "N" designates the number of HTDMA scans used in the fit routine. The first row for each composition shows results for the fit routine run without added random error, the second row of results for the same data pair represents average results of 20 runs of the fit routine with assumed random error added to the input data pairs. Ratios of standard deviations in predicted values of S_{crit} to average values of S_{crit} were less than 0.16 for the cases with applied errors. Errors in S_{crit} and D_{crit} are calculated relative to theoretical values from the reference Köhler model.

Compound	N	$D_{p,sol}$ (nm)	Y_f	$\beta_{0,f}$	S_{crit} (%)	S_{crit} Err. (%)	D_{crit} (nm)	Error D_{crit} (%)	χ^2
NaCl	19	37	84.767	0.01611	0.42	−21	321	12	0.0800
NaCl		37	93.656	0.01114	0.40	−24	334	17	1.04
NaCl	12	46	45.787	0.08943	0.40	6	337	−15	2.44
NaCl		46	55.641	0.06072	0.36	−6	379	−5	1.73
NaCl	8	44	65.292	0.03302	0.37	−10	368	0	1.31
NaCl		44	67.561	0.03248	0.36	−11	372	0	0.981
$(NH_4)_2SO_4$	43	57	33.353	0.00247	0.35	−13	388	5	1.72
$(NH_4)_2SO_4$		57	34.225	0.00101	0.33	−16	403	9	2.35
NH_4HSO_4	30	40	31.289	0.00596	0.62	−16	217	5	2.51
NH_4HSO_4		40	33.059	0.00398	0.61	−18	222	8	3.21

TABLE 3. Summary of theoretical S_{crit} values, Y_f and $\beta_{0,f}$ fit parameters, and D_{crit} values determined HTDMA study results on particles composed of internally and externally mixed particles and ambient particles of unknown chemical composition. The confidence interval of HTDMA-derived values of S_{crit} is ±28%. ''N'' designates the number of HTDMA scans used in the fit routine. The first row for each composition shows results for the fit routine run without added random error, the second row of results for the same data pair represents average results of 20 runs of the fit routine with assumed random error added to the input data pairs. Ratios of standard deviations in predicted values of S_{crit} to average values of S_{crit} were less than 0.16 for the cases with applied errors. Errors in S_{crit} and D_{crit} are calculated relative to theoretical values from the reference Köhler model. ''Emix'' designates results from externally mixed studies and ''Imix'' those from internally mixed studies. Results from the two externally mixed studies have been combined and results from NaCl and $(NH_4)_2SO_4$ particles are reported separately.

Compound	N	$D_{p,sol}$ (nm)	Y_f	$\beta_{0,f}$	S_{crit} (%)	S_{crit} Err. (%)	D_{crit} (nm)	Error D_{crit} (%)	χ^2
Imix	17	32	37.791	0.05239	0.78	10	175	5	2.11
Imix		32	53.002	0.02558	0.65	−8	207	25	2.51
Emix	34	40	39.751	−0.00141	0.55	−22	245	16	3.16
$(NH_4)_2SO_4$		40	41.757	−0.00242	0.54	−23	249	18	3.76
Emix	34	37	90.184	0.01185	0.41	−24	330	15	1.72
NaCl		37	96.198	0.00919	0.40	−25	337	18	2.01
Ambient	19	85	8.824	−0.00404	0.37	−27			4.21
Ambient		85	9.332	−0.00450	0.35	−32			3.54
Ambient	14	68.4	10.743	−0.00444	0.47	−6			10.35
Ambient		68.4	10.808	−0.00434	0.47	−6			10.05
Ambient	18	120	13.617	−0.00260	0.18	−65			4.44
Ambient		120	13.772	−0.00299	0.18	−65			4.61

theoretical values were predicted by the fit routine when the total RH range of the input data was smaller than 6% RH. The worse agreement is the result of having an insufficient number of data pairs to capture the curvature in Eq. (1).

d. Comparison of measured, HTDMA-derived, and theoretical values of S_{crit} for internally and externally mixed particles

The proposed method for deriving S_{crit} from HTDMA results was applied to equimolar, internally mixed particles of NaCl and $(NH_4)_2SO_4$. Internally mixed particles represent a more stringent test of the proposed method for deriving S_{crit} from HTDMA results compared to runs with single solutes, as internally mixed particles dissociate into three or more ions, whereas the model is explicitly written only for solutes that dissociate into two ions. A shape factor of 1.25 was applied to the dry particle size selected by DMA1 so that experimental growth would match theoretically predicted growth; the average percent difference was 0.7% ± 1.2%. The use of a shape factor is supported by transmission electron micrographs of deposited particles showing that they were of irregular shape with protrusions. The micrographs did not allow a quantitative assessment of the shape factor to be made, but qualitatively supported the need for a shape factor; the chosen factor is between that for a cubic structure (1.08) and quartz (1.36; Hinds 1982). Results from the fit of Eq. (1) to the internally mixed particle growth results are listed in Table 3 using the same format as in Table 2. The average agreement between HTDMA-derived and theoretical values of S_{crit} is between −8% and 10%, with a standard deviation of 10% in the values of S_{crit} from the 20 runs with applied errors. The agreement between derived and theoretical values of Y_f is −23% for the case with no applied errors and 8% for the case with applied errors. The agreement is similar to differences in the magnitudes of values of Y_f for internally mixed NaCl–$(NH_4)_2SO_4$ and $(NH_4)_2SO_4$ or NH_4HSO_4 compositions, but smaller than the differences between values of Y_f for internally mixed NaCl–$(NH_4)_2SO_4$ and NaCl. The similarity between derived and theoretical values of Y_f for internally mixed particles suggests that the modified Köhler model is capable of predicting Y_f values for the more complex composition. We note, however, that only one study of internally mixed particles was conducted involving 17 HTDMA scans. For the one CCN study conducted on 32-nm internally mixed NaCl–$(NH_4)_2SO_4$ particles, the agreement between CCNC-derived and theoretical values of S_{crit} was −8%. We note that the theoretical critical supersaturation of an internally mixed $(NH_4)_2SO_4$–NaCl particle without the applied shape factor (i.e., 40-nm diameter) is 40% lower than the value of S_{crit} determined from the CCN study on internally mixed particles and the value predicted by the fit routine.

Externally mixed particles were created by operating two atomizers in parallel and combining their output flows in the dilution and drying chamber so that approximately equal number concentrations of each composition was present. One atomizer was operated with an $(NH_4)_2SO_4$ solution and the second atomizer with an NaCl solution. A shape factor of 1.08 was applied to the NaCl dry particle size selected by DMA1, as described previously. Two growth modes were observed in the HTDMA, clearly demonstrating that particles of different chemical composition sampled simultaneously could be distinguished based on differences in their hygroscopic growth. The results from two such studies are shown in Table 3. For each of the two studies, a dry particle size of 40 nm was selected with the first DMA, and results have been combined in Table 3. The agree-

ment between experimental and theoretical growth was very good for both solutes. The average percent difference between theoretical and experimental hygroscopic growth was 1.3% ± 0.7% for NaCl and 0.7% ± 1.4% for $(NH_4)_2SO_4$.

The average agreement between experimentally derived and theoretical values of S_{crit} in Table 3 for the externally mixed particle studies is −23% (1 σ = 5%, n = 34) for $(NH_4)_2SO_4$ and −25% (1 σ = 6%, n = 34) for NaCl. The poorer average agreement is reflected in the larger average χ^2 values in Table 3 compared to previous studies on $(NH_4)_2SO_4$ and NaCl particles. The values of Y_f in Table 3 derived from the fit routine for $(NH_4)_2SO_4$ and NaCl are clearly different. This demonstrates that the technique for deriving S_{crit} from HTDMA results can differentiate between particles with different chemical compositions sampled at the same time. The percent difference between HTDMA-derived and theoretical S_{crit} values is larger than for other studies. The differences are close to the ±22% confidence interval in values of S_{crit} derived from CCN studies. The individual values of S_{crit} corresponding to the externally mixed NaCl–$(NH_4)_2SO_4$ particles could not be distinguished by the CCN counter. Interestingly, the agreement between the experimentally determined value of S_{crit} and the average of the theoretical values of S_{crit} for 40-nm $(NH_4)_2SO_4$ and 37-nm NaCl particles was extremely good, within −7%.

e. Comparison of measured, HTDMA derived, and theoretical values of S_{crit} for ambient particles

Ambient air samples were drawn from above the roof of the laboratory through a 1.2-cm inside diameter, electrically conductive, plastic sampling line 8 m long. We note that ambient studies were conducted on three different monodisperse particle populations on three different days (one size per day). The flow rate in the inlet tubing was 8 L min^{-1}. No dilution air was added to the ambient sample, as the monodisperse particle concentrations were already significantly lower than during laboratory studies of atomized salt particles. The particle sample was drawn into DMA1 through a diffusion dryer and the operation of other components of the HTDMA–CCN system was analogous to studies on atomized salt particles. The relative humidity of the DMA1 sample inlet flow was between 2% and 9% for all studies on ambient particles. Hygroscopic growth results for ambient particles are shown in Fig. 6. A shape factor is likely required for the sampled particles; however, we have no way of estimating an appropriate value and electron micrograph grid samples were not collected; thus the particles were assumed to be spherical. Data pairs have been numbered for later reference. Three studies of ambient particles were conducted on DOYs 174 (solid dots), 175 (asterisks), and 182 (squares). The particle size selected by DMA1 was different for the three studies: 85-nm-diameter particles were selected on

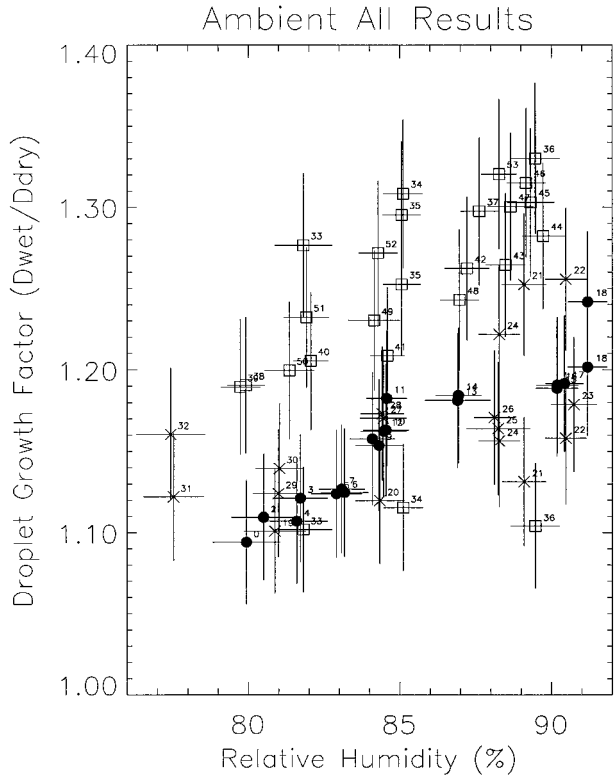

FIG. 6. As in Fig. 2 except for three studies on ambient particles. Results from DOY 182 designated by squares, results from DOY 174 designated by solid dots, and DOY 175 results are shown as asterisks.

DOY 174, 68.4-nm particles were examined on DOY 175, and 120-nm particles were selected on DOY 182. Local meteorological data were collected at the Colorado State University (CSU) Department of Atmospheric Science Christman Field meteorological data station, located approximately 100 m from the sample inlet. Time lines of concentrations of monodisperse particles observed by the UCPC have been plotted in Fig. 7 to help interpret changes in the observed hygroscopic growth. The average monodisperse particle concentrations on DOYs 174, 175, and 182 were 34.5, 22.1, and 48.1 cm^{-3}, corresponding to 85-, 68.4-, and 120-nm dry particle diameters, respectively. However, concentrations reached 80 cm^{-3} on DOY 182, whereas maximum concentrations were only 60 cm^{-3} during the other two studies. Highest concentrations occurred during periods where winds were easterly and light and when winds were from the south, consistent with the relative locations of anthropogenic sources of particles. Lowest concentrations were observed when winds were high and from the west and northwest. The most obvious change in UCPC concentration occurred at DOYs 175.57 and 182.8 (Fig. 7). It is possible that the variability in the number concentration on DOY 182 adversely affected the value of S_{crit} derived from CCN studies.

A striking feature of the results from the ambient studies is the much lower observed growth compared

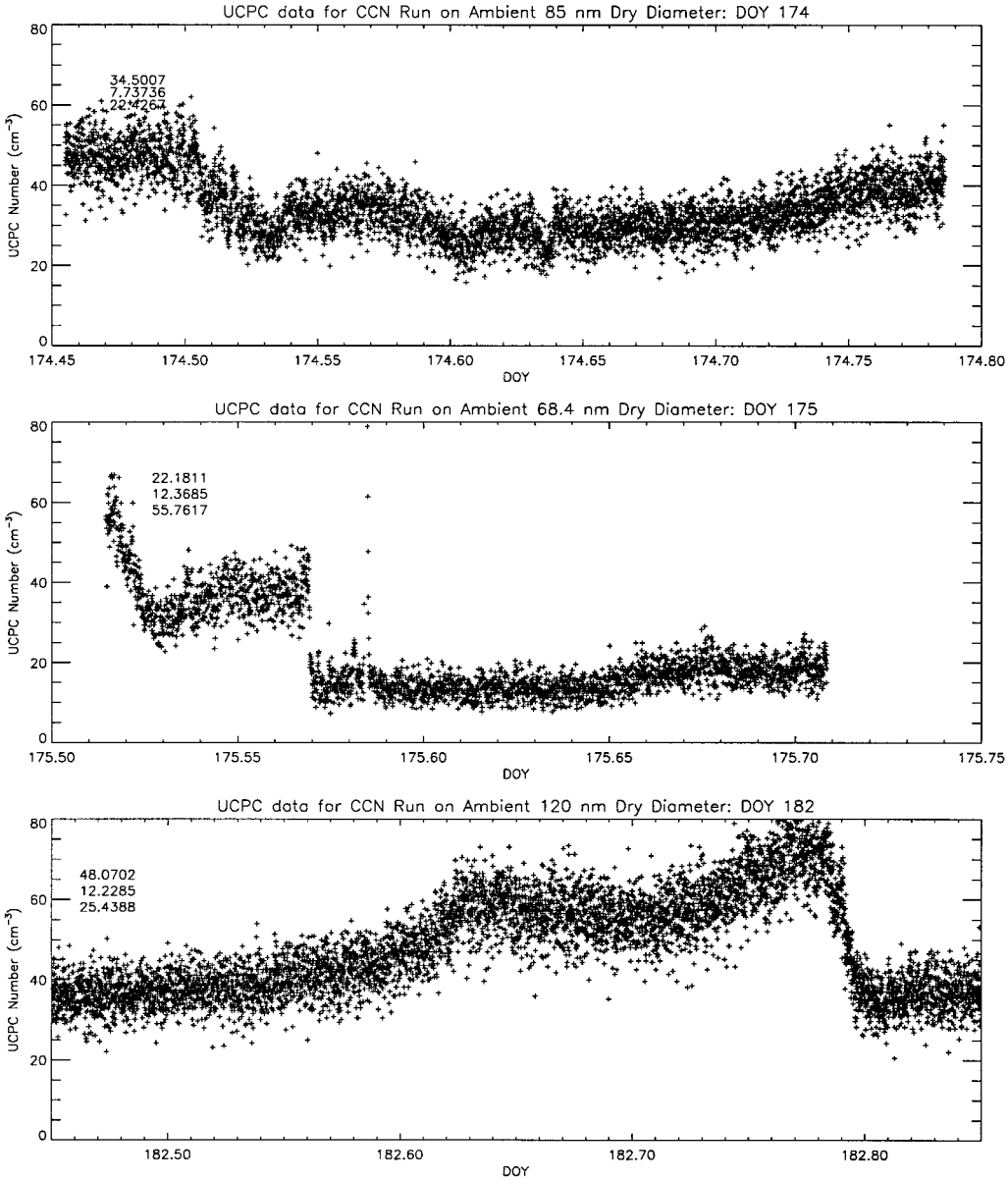

FIG. 7. UCPC monodisperse number concentrations during all studies on ambient particles. Average number concentration, standard deviation, and coefficient of variation (%) are arranged in a column from top to bottom in each plot.

with pure salts. The $(NH_4)_2SO_4$ and NaCl particles exhibit growth that is between 26% and 52% greater at 80% RH and between 21% and 72% greater at 90% RH than the largest growth factors observed for ambient samples. Assuming that the particle chemical compositions were similar on the three days, the results also suggest that when only a single hygroscopic mode was observed larger particles (120 nm, squares) were more hygroscopic than smaller particles (other symbols). Larger particles were also found to be more hygroscopic in HTDMA studies by McMurry and Stolzenburg (1989) in the Los Angeles area.

Of the 54 total HTDMA scans conducted, two distinct growth modes were discerned in eight. Of these eight cases, only one was observed on DOY 174, at the highest study RH (data pair 18, DOY 174.76); three were observed at the highest RHs examined on DOY 175 (data pairs 21, 22, and 24, DOY 175.57–175.61); and four were observed at RHs between 81% and 90% on DOY 182 (data pairs 33, 34, and 36, DOY 182.49–182.54). On DOY 182, two distinct growth modes were observed in the first four HTDMA scans at RHs between 82% and 90%, but not during HTDMA scans at these same RHs later in the study (i.e., data pairs 40–53, DOY

182.6–182.85). When two growth modes were observed, there appeared to be a larger difference between the growth factors of the two modes for the larger particles compared to the smaller particles.

Although the chemical composition of the ambient particles was unknown, possible compositions were examined by assuming the sampled particles consisted of internal mixtures of $(NH_4)_2SO_4$, NH_4NO_3, and an insoluble compound. The insoluble compound was assumed to have a dry density of 1000 kg m^{-3} and a molecular weight of 40 g mol^{-1}. A full Köhler model for an aqueous solution drop containing a solid insoluble substance was used to calculate the equilibrium RHs for the sample particle compositions (Pruppacher and Klett 1997). The choice of soluble compounds is supported by filter and impactor sampling results from earlier studies of ambient particles along the Front Range of Colorado that showed $(NH_4)_2SO_4$ and NH_4NO_3 were present. Equilibrium RHs were calculated as a function of droplet size for various mass fractions of the three constituents and the particle sizes selected during each of the three ambient studies. Curves of RH versus D_{drop} were compared to observed (RH, D_{drop}) data pairs for each ambient study. The mass fraction values that provided the best fit, determined visually, to observed (RH, D_{drop}) data pairs were used to calculate S_{crit} values for each ambient study. For the studies on DOYs 174 and 175, the same combination of the three compounds provided a reasonable fit to observed droplet growth factors. For these studies, the mass fractions of $(NH_4)_2SO_4$, NH_4NO_3, and insoluble material were 0.14, 0.09, and 0.77, respectively. Therefore, the volume fraction of soluble material in the sampled particles is estimated to be only 14%. We note, however, that the estimated mass fractions of the three compounds are probably not unique since different combinations of species and insoluble matter could also fit the observed droplet growth factors. The calculated values of S_{crit} for the assumed chemical compositions on DOYs 174 and 175 differ from values derived from CCN studies by 10% and −23%, respectively. This level of agreement is similar to that found in other CCN studies of this work. For the study on DOY 182, a different mixture of compounds best simulated the observed hygroscopic behavior. The mass fractions of $(NH_4)_2SO_4$, NH_4NO_3, and insoluble material were 0.25, 0.15, and 0.6, respectively. The estimated volume fraction of soluble material in the 120-nm-diameter particles is 27%. Correspondingly, the predicted value of S_{crit} for DOY 182 is 0.2%, much lower than the value of 0.53% derived from CCN studies. The hypothetical value of S_{crit} derived for the assumed chemical composition agrees very well with the value from the fit routine for this study (0.18%). Svenningson et al. (1994) used their HTDMA results to estimate the volume fraction of soluble material in particles at a continental sampling site. They found that values of the soluble fraction varied between 2% for less hygroscopic particles with growth factors less than 1.11 and 53% for more hygroscopic particles with growth factors around 1.35. The soluble fraction and growth factor values are in reasonable agreement with the corresponding values of this work.

The RH, D_{drop} pairs were used in the fit routine to derive S_{crit} for ambient particles, and results are listed in Table 3. For the eight cases where two hygroscopic modes were observed in a single scan, the more hygroscopic mode was chosen to be used in the fit routine. The values of Y_f derived for the ambient particle samples are also shown in Table 3. It is of interest to note that most of the values are between two and ten times smaller than those derived for the pure salts, consistent with the lower observed hygroscopic growth of the ambient particles compared to the salts. For the three studies, the average agreement between values of S_{crit} derived from CCN studies and values of S_{crit} derived from HTDMA results is −38% with a standard deviation of 5%. Furthermore, the χ^2 values of the fits listed in Table 3 are generally larger than those from studies on known salts, indicating that the modified Köhler model does not simulate the growth of ambient particles as well as particles composed of the other compositions examined in this work. The largest error, −65%, was found for the study on 120-nm particles (DOY 182) and may be due to the variability in number concentration during the study. As mentioned above, the calculated value of S_{crit} for a hypothetical chemical composition exhibiting droplet growth similar to that observed on DOY 182 is closer to the value predicted from the fit routine than to the value from CCN studies. The percent difference between HTDMA-derived and CCNC-derived S_{crit} values is larger than the −0.6% ($1\ \sigma = 11\%$, $n = 16$) uncertainty in S_{crit} values derived from CCN studies on known composition particles. For the study on 68.4-nm particles on DOY 175, the agreement between HTDMA-derived (0.47%) and CCN-derived (0.5%) values of S_{crit} is much better: −6%, closer to the experimental uncertainty in the value of S_{crit}. Studies of the influence of the choice of data pair subsets on predicted values of S_{crit} again demonstrated that a 7% RH range was too small to derive accurate values of S_{crit}. A 10% RH range was found to produce better predicted values of S_{crit}.

In addition to the variability of the particle properties during the studies, the poor performance of the model on the ambient data may be because the particles were composed of internal mixtures of materials that did not fully dissociate in solution or somehow inhibited the condensation process. Limitations in the current, modified Köhler model may preclude the prediction of accurate values of S_{crit} from HTDMA results for ambient particles of unknown composition. For example, it is possible that an additional adjustable parameter, for example, the insoluble fraction, would improve the ability of the model to capture the curvature of Eq. (1). Another possibility is that certain surface-active organic compounds influenced the critical supersaturation by inhibiting the uptake of water (Schulmann et al. 1996); this

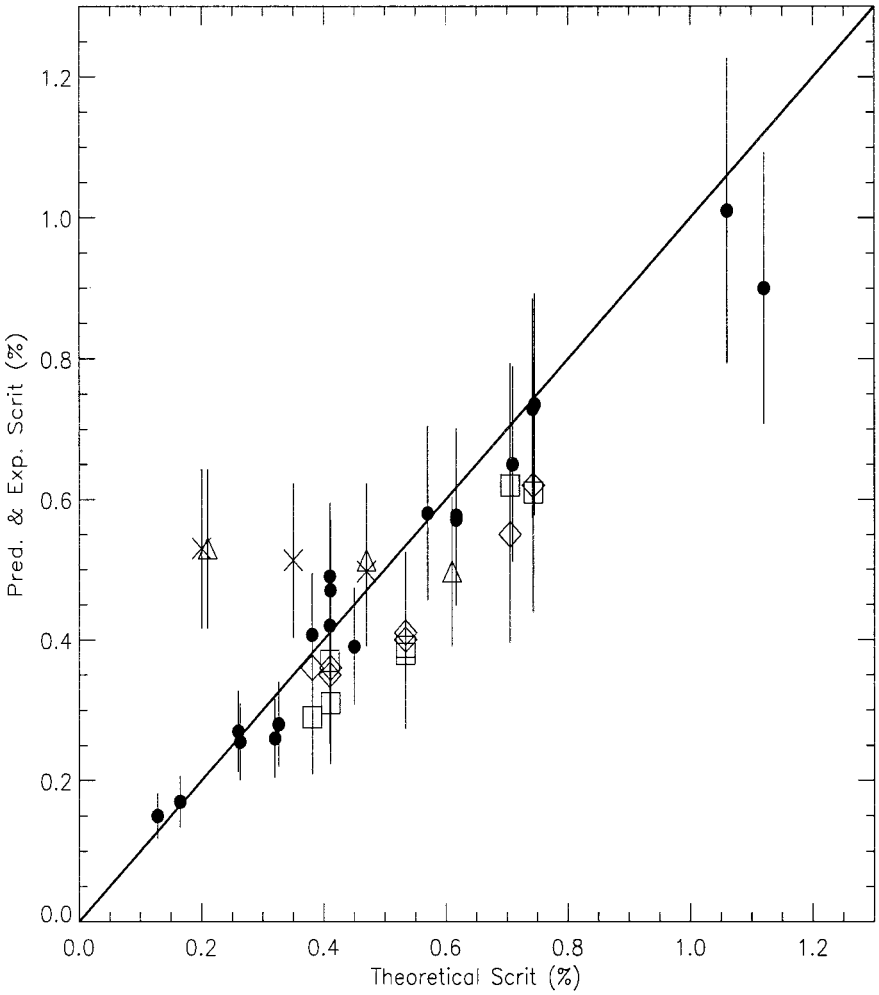

FIG. 8. Comparison of values of S_{crit} derived from CCN studies (solid dots), the fit technique with the Köhler model in this work (diamonds), and the fit technique with the Köhler model from Weingartner et al. (1997) (squares), for all compounds studied in this work. The solid line designates perfect agreement between experimental and theoretical values of S_{crit}. The "×" designates results for ambient samples and the model of this work, triangles designate ambient results from the model of Weingartner et al. (1997). Results from ambient studies are plotted as the CCNC-derived value of S_{crit} on the *y* axis and the HTDMA-derived value of S_{crit} on the *x* axis. The confidence interval for CCNC-derived values of S_{crit} is ±22% while that for HTDMA-derived values is ±28%.

effect is not accounted for in our model. More studies on ambient particles are required to better quantify model limitations, however, the general applicability of Pitzer's model of the osmotic coefficient provides some confidence that a new parameterization could be developed so that S_{crit} could be successfully derived for ambient particles.

f. Summary of HTDMA-derived values of S_{crit} and comparison with a simpler Köhler model

The values of S_{crit} predicted by the model in this work (diamonds) are compared to CCNC-derived values (solid dots) in Fig. 8 for all of the particle types studied here. The HTDMA-derived values of S_{crit} in Fig. 8 are predicted using all of the HTDMA study results for each compound with applied error. The solid dots shown are the same data plotted in Fig. 5. The simpler Köhler model proposed by Weingartner et al. (1997) discussed in Part I of this work was also fit to HTDMA data, with derived values of S_{crit} shown as squares in Fig. 8. The "×" symbols in Fig. 8 designate ambient study results from the model of this work and triangles represent results from the model of Weingartner et al. (1997) for ambient studies. The HTDMA-derived value of S_{crit} are plotted as the abscissa and the CCNC-derived value of S_{crit} as the ordinate. It is worth noting that for studies involving dry particle diameters between 32 and 40 nm, the various chemical compositions examined represent a factor of 2 change in S_{crit}, demonstrating that both

chemical composition and particle size are important factors in determining S_{crit}. Results in Fig. 8 demonstrate good agreement between HTDMA-derived, CCNC-derived, and theoretical values of S_{crit}. The average agreement between theoretical and predicted values of S_{crit} for particles of known chemical composition is -20% ($1\ \sigma = 8\%$, $n = 7$) for the model proposed by Weingartner et al. (1997) and -16% ($1\ \sigma = 7\%$, $n = 7$) for the model of this work. On average, both methods for predicting S_{crit} from HTDMA results tend to underpredict values of S_{crit} over the supersaturation range examined.

As shown in Part I, assumptions made in the modified Köhler model result in underpredictions of values of the Kelvin term and overpredictions of Φ, which in turn result in underpredictions of values of RH and S_{crit}. For many of the particles composed of single solutes studied here, the osmotic coefficient varies between values slightly above 1 and values slightly below 1 (NaCl) or is less than 1 [$(NH_4)_2SO_4$, NH_4HSO_4, NH_4NO_3, internally mixed solutes] for the RH range and molalities experienced during HTDMA studies (1–6 molal). For example, for $(NH_4)_2SO_4$ the osmotic coefficient is near 0.75 for molalities greater than 6 molal, decreases to 0.65 for molalities between 6 and 1, and then exponentially approaches unity as the molality decreases below 1 molal. In the model of Weingartner et al. (1997) the product $\nu\rho_s\Phi/M_s$ is assumed to be constant as the one free fit parameter in the model (N_i). Therefore, the assumption is made that Φ does not vary with RH. As mentioned above, for HTDMA conditions and many of the compounds studied here, the osmotic coefficient value does not vary significantly, and the simpler model of Weingartner et al. (1997) can do a reasonable job of predicting S_{crit} if measurements are made in the appropriate molality range. However, in general, compounds do not have osmotic coefficient values that are constant for droplet molalities experienced during HTDMA measurements. A good example is NH_4NO_3, where the osmotic coefficient demonstrates a monotonic decrease from a value of 0.8 for a 1-molal solution, to a value of 0.65 for a 6-molal solution. Correspondingly, as shown in Part I, the model of Weingartner et al. (1997) exhibited a larger error in predicted S_{crit} in numerical studies on particles composed of NH_4NO_3.

4. Conclusions

A technique for using hygroscopic growth measurements at RHs $< 100\%$ to derive the critical supersaturation required to activate a particle to a cloud droplet has been applied to measurements of droplet growth for particles composed of NaCl, $(NH_4)_2SO_4$, NH_4HSO_4, internally mixed NaCl–$(NH_4)_2SO_4$, externally mixed NaCl–$(NH_4)_2SO_4$, and ambient particles of unknown composition. Operation of the HTDMA was validated by comparing observed hygroscopic growth with published data. The errors in observed hygroscopic growth factors for particles composed of NaCl and $(NH_4)_2SO_4$ were calculated to be less than $\pm 1.7\%$. By applying the necessary loss corrections to the input particle number concentrations, systematic studies on particles of known size and chemical composition have demonstrated that a thermal gradient diffusion chamber CCN counter can be used to determine the critical supersaturation of monodisperse particles within -0.6% of theoretical values with a standard deviation of 11% ($n = 16$). The confidence interval in CCNC-derived values of S_{crit} was $\pm 22\%$ at the 95% confidence level.

A modified Köhler model including a parameterization for the solution osmotic coefficient that approaches the correct thermodynamic limit was fitted to experimental growth results in order to derive two composition-dependent unknowns, Y_f and $\beta_{0,f}$. Only 30–60 min are required to acquire the data necessary to derive a value of S_{crit} from HTDMA study results. HTDMA-derived values of S_{crit} for particles composed of NaCl, $(NH_4)_2SO_4$, and NH_4HSO_4 agree with theoretical values to within -13% ($\sigma = 8.5\%$, $n = 8$). The 95% confidence interval in HTDMA-derived values of S_{crit} was $\pm 28\%$. The agreement between the theoretical, CCNC-derived, and HTDMA-derived values of S_{crit} demonstrates that the proposed technique can derive accurate values of S_{crit} from hygroscopic growth data for the particle types studied here.

Values of S_{crit} were also derived from HTDMA study results using the Köhler model proposed by Weingartner et al. (1997). Slightly better agreement was found between theoretical and predicted values of S_{crit} from the model of this work than values predicted by the model of Weingartner et al. (1997). The S_{crit} values from CCN studies did not agree within experimental uncertainties with those derived from either model applied to HTDMA data from two of the three ambient particle studies conducted for this work. The poorer agreement for the ambient studies is believed to be due to the variability in ambient particle concentration and chemical composition during the study, the low number concentrations of particles that were available to be sampled, and the likely complex mixture of more and less hygroscopic material in the ambient particles resulting in hygroscopic behavior that could not be captured by the modified Köhler model. The presence of slightly soluble compounds, for example, $CaSO_4$ or some organic acids, can alter S_{crit} through changes to the droplet solution surface tension and by the presence of an undissolved, insoluble, or slightly soluble core (Schulmann et al. 1996; Laaksonen et al. 1998). These effects are likely to be important for ambient particles and are not accounted for in the current version of the modified Köhler theory. Furthermore, as pointed out by Laaksonen et al. (1998), the presence of soluble gases could decrease the values of S_{crit} of particles sampled by the CCN counter, and this effect would not be accounted for in the modified Köhler model used to determine the HTDMA-derived values of S_{crit}. An additional adjust-

able parameter in the model that accounts for the presence of insoluble material may improve the accuracy of HTDMA-derived values of S_{crit} for ambient particles. Future work will include more studies of ambient particles of unknown composition and the development of an improved Köhler model explicitly accounting for the presence of partially soluble and insoluble material in sampled particles.

Acknowledgments. This work was sponsored by the Environmental Protection Agency under STAR Graduate Fellowship U-914726-01-0. W. R. Leaitch is thanked for the loan of the CCN counter. The assistance of S. N. Pandis and C. N. Cruz with the CCN counter operation was much appreciated. The comments of J. Hudson and one anonymous reviewer are greatly appreciated.

REFERENCES

Berg, O. H., E. Swietlicki, and R. Krejci, 1998: Hygroscopic growth of aerosol particles in the marine boundary layer over the Pacific and Southern Oceans during ACE 1. *J. Geophys. Res.,* **103,** 16 535–16 545.

Brechtel, F. J., and S. M. Kreidenweis, 2000: Predicting particle critical supersaturation from hygroscopic growth measurements in the humidified TDMA. Part I: Theory and sensitivity studies. *J. Atmos. Sci.,* **57,** 1854–1871.

Covert, D. S., J. L. Gras, A. Wiedensohler, and F. Stratmann, 1998: Comparison of directly measured CCN with CCN modeled from the number-size distribution in the MBL during ACE-1 at Cape Grim. *J. Geophys. Res.,* **103,** 16 597–16 608.

Cruz, C. N., and S. N. Pandis, 1997: A study of the ability of pure secondary organic aerosol to act as cloud condensation nuclei. *Atmos. Environ.,* **31,** 2205–2214.

Fitzgerald, J. W., W. A. Hoppel, and M. A. Vietti, 1982: The size and scattering coefficient of urban aerosol particles at Washington, D.C. as a function of relative humidity. *J. Atmos. Sci.,* **39,** 1838–1852.

Greenspan, L., 1977: Humidity fixed points of binary saturated aqueous solutions. *J. Res. Nat. Bur. Stand., Sect. A:* **81A,** 89–95.

Hinds, W. C., 1982: *Aerosol Technology: Properties, Behavior, and Measurement of Airborne Particles.* John Wiley and Sons, 424 pp.

Hudson, J. G., 1982: Correlation between surface and cloud base CCN spectra in Montana. *J. Appl. Meteor.,* **21,** 1427–1440.

——, Y. Xie, and S. S. Yum, 1998: Vertical distributions of cloud condensation nuclei spectra over the summertime Southern Ocean. *J. Geophys. Res.,* **103** (D13), 16 609–16 624.

Kelly, W. P., and P. H. McMurry, 1992: Measurement of particle density by inertial classification of differential mobility analyzer-generated monodisperse aerosols. *Aerosol Sci. Tech.,* **17,** 199–212.

Kim, Y. P., J. H. Seinfeld, and P. Saxena, 1993: Atmospheric gas-aerosol equilibrium. I. Thermodynamic model. *Aerosol Sci. Tech.,* **19,** 157–181.

Kinney, P. D., D. Y. H. Pui, W. Mulholland, and N. P. Bryner, 1991: Use of the electrostatic classifier method to size 0.1 mm SRM particles—A feasibility study. *J. Res. Nat. Inst. Stand. Techn.,* **96,** 147–175.

Laaksonen, A., P. Korhonen, M. Kulmala, and R. J. Charlson, 1998: Modification of the Köhler equation to include soluble trace gases and slightly soluble substances. *J. Atmos. Sci.,* **55,** 853–862.

Pitzer, K. S., and G. Mayorga, 1973: Thermodynamics of electrolytes. II. Activity and osmotic coefficients for strong electrolytes with one or both ions univalent. *J. Phys. Chem.,* **77,** 2300–2308.

Pruppacher, H. R., and J. D. Klett, 1997: *Microphysics of Clouds and Precipitation.* Dordrecht Publishers, 954 pp.

Rader, D. J., and P. H. McMurry, 1986: Application of the tandem differential mobility analyzer to studies of droplet growth or evaporation. *J. Aerosol Sci.,* **17,** 771–787.

Schulmann, M. L., M. C. Jacobsen, R. J. Charlson, R. E. Synovec, and T. E. Young, 1996: Dissolution behavior and surface tension effects of organic compounds in nucleating cloud droplets. *Geophys. Res. Lett.,* **23,** 277–280.

Skoog, D. A., D. M. West, and F. J. Holler, 1992: *Fundamentals of Analytical Chemistry*. 6th ed. Saunders College Publishing, 1255 pp.

Svenningsson, B., H.-C. Hansson, A. Wiedensohler, K. Noone, J. Ogren, A. Hallberg, and R. Colville, 1994: Hygroscopic growth of aerosol particles and its influence on nucleation scavenging in cloud: Experimental results from Kleiner Feldberg. *J. Atmos. Chem.,* **19,** 129–152.

Tang, I. N., and H. R. Munkelwitz, 1994: Water activities, densities, and refractive indices of aqueous sulfates and sodium nitrate droplets of atmospheric importance. *J. Geophys. Res.,* **99,** 18 801–18 808.

Weingartner, E., H. Burtscher, and U. Baltensperger, 1997: Hygroscopic properties of carbon and diesel soot particles. *Atmos. Environ.,* **31,** 2311–2327.

Wiedensohler, A., 1988: An approximation of the bipolar charge distribution for particles in the submicron size range. *J. Aerosol. Sci.,* **19,** 387–389.